ACCOUNTS
of chemical research

The Roles of Entropy and Enthalpy in Stabilizing Ion-Pairs at Transition States in Zeolite Acid Catalysis

RAJAMANI GOUNDER AND ENRIQUE IGLESIA*

Department of Chemical Engineering, University of California at Berkeley, Berkeley, California 94720, United States

RECEIVED ON MAY 17, 2011

CONSPECTUS

Acidic zeolites are indispensable catalysts in the petrochemical industry because they select reactants and their chemical pathways based on size and shape. Voids of molecular dimensions confine reactive intermediates and transition states that mediate chemical reactions, stabilizing them by van der Waals interactions. This behavior is reminiscent of the solvation effects prevalent within enzyme pockets and has analogous consequences for catalytic specificity. Voids provide the "right fit" for certain transition states, reflected in their lower free energies, thus extending the catalytic diversity of zeolites well beyond simple size discrimination. This catalytic diversity is even more remarkable because acid strength is essentially unaffected by confinement among known crystalline aluminosilicates. In this Account, we discuss factors that determine the "right fit" for a specific chemical reaction, exploring predictive criteria that extend the prevailing discourse based on size and shape. We link the structures of reactants, transition states, and confining voids to chemical reactivity and selectivity.

Confinement mediates enthalpy–entropy compromises that determine the Gibbs free energies of transition states and relevant reactants; these activation free energies determine turnover rates via transition state theory. At low temperatures (400–500 K), dimethyl ether carbonylation occurs with high specificity within small eight-membered ring (8-MR) voids in FER and MOR zeolite structures, but at undetectable rates within larger voids (MFI, BEA, FAU, and SiO_2–Al_2O_3). More effective van der Waals stabilization within 8-MR voids leads to lower ion-pair enthalpies but also lower entropies; taken together, carbonylation activation free energies are lower within 8-MR voids. The "right fit" is a "tight fit" at low temperatures, a consequence of how temperature appears in the defining equation for Gibbs free energy.

In contrast, entropy effects dominate in high-temperature alkane activation (700–800 K), for which the "right fit" becomes a "loose fit". Alkane activation turnovers are still faster on 8-MR MOR protons because these transition states are confined only partially within shallow 8-MR pockets; they retain higher entropies than ion-pairs fully confined within 12-MR channels at the expense of enthalpic stability. Selectivities for *n*-alkane dehydrogenation (relative to cracking) and isoalkane cracking (relative to dehydrogenation) are higher on 8-MR than 12-MR sites because partial confinement preferentially stabilizes looser ion-pair structures; these structures occur later along reaction coordinates and are higher in energy, consistent with Marcus theory for charge-transfer reactions. Enthalpy differences between cracking and dehydrogenation ion-pairs for a given reactant are independent of zeolite structure (FAU, FER, MFI, or MOR) and predominantly reflect the different gas-phase proton affinities of alkane C–C and C–H bonds, as expected from Born–Haber thermochemical cycles. These thermochemical relations, together with statistical mechanics-based treatments, predict that rotational entropy differences between intact reactants and ion-pair transition states cause intrinsic cracking rates to increase with *n*-alkane size.

Through these illustrative examples, we highlight the effects of reactant and catalyst structures on ion-pair transition state enthalpies and entropies. Our discussion underscores the role of temperature in mediating enthalpic and entropic contributions to free energies and, in turn, to rates and selectivities in zeolite acid catalysis.

10.1021/ar200138n

Introduction

Zeolites are used in refining and petrochemical processes as Brønsted acid catalysts that target specific products based on the relative sizes and shapes of the molecules and confining voids.[1−3] Cracking, alkylation, and hydride transfer reactions require that ion-pairs form at transition states from relatively uncharged physisorbed reactants or bound alkoxides.[3−7] Activation barriers decrease as ion-pairs become more stable with increasing acid strength, reflected in smaller deprotonation energies (ΔE_{DP}), and with smaller cation−anion distances.[5−7] In contrast, activation barriers for steps involving more neutral transition states that are predominantly stabilized by covalent interactions, such as H−D exchange and alkene adsorption, depend weakly on acid strength.[5−7]

Brønsted acid sites within aluminosilicates are weaker (ΔE_{DP} ~1200 kJ/mol) than in Brønsted−Lewis superacids (HF-SbF_5; ΔE_{DP} ~1000 kJ/mol),[8] polyoxometalates, or anion-modified oxides (ΔE_{DP} ~1050−1150 kJ/mol).[9] Theoretical treatments of structural and electrostatic effects in zeolite frameworks indicate that ΔE_{DP} values are similar for isolated protons (within ~10 kJ/mol) at all locations within MFI[10] and MOR[11] and for the most stable locations in other frameworks.[12] Even though acid sites in zeolites are weaker and less diverse in composition and strength than in mesoporous or liquid acids, turnover rates are often higher than those on stronger acids and depend sensitively on the geometry of both the microporous voids and the reacting molecules.[13−16]

Confinement causes ubiquitous compromises between entropy and enthalpy because dispersion forces restrict mobility. Smaller channels confine alkanes (and transition states by extension) more strongly *as long as they fit*, because more effective van der Waals contacts with framework O-atoms make adsorption enthalpies and entropies more negative.[17−20] Chemical reaction rates depend on the Gibbs free energies of transition states ($\Delta G^\circ_\ddagger$) with respect to the relevant reactants.

$$\Delta G^\circ_\ddagger = \Delta H^\circ_\ddagger - T\Delta S^\circ_\ddagger \quad (1)$$

Thus, trade-offs between enthalpy ($\Delta H^\circ_\ddagger$) and entropy ($\Delta S^\circ_\ddagger$) upon confinement determine reactivity. Enthalpic contributions tend to dominate at low temperatures, for which the first term in eq 1 prevails, while entropic effects become important at higher temperatures. In turn, we expect that stronger solvation and a tighter fit will benefit chemical reactivity at low temperatures, but that a looser fit will do so at higher temperatures. We illustrate these trends for alkane cracking and dehydrogenation at high temperatures (700−800 K), where entropy effects prevail and vary predictably with alkane structure and with the lateness of transition states along reaction coordinates. In sharp contrast, enthalpic considerations dominate free energies at the low temperatures (400−500 K) of dimethyl either (DME) carbonylation.

Enthalpic Stabilization and "Tighter Fits" in Carbonylation Catalysis

DME carbonylation under anhydrous conditions selectively forms methyl acetate on acidic zeolites at 400−500 K via kinetically-relevant addition of CO to bound CH_3 groups.[21−23] Turnover rates are much higher on zeolites containing eight-membered ring (8-MR) structures (FER, MOR) than on materials with larger voids (MFI, BEA, FAU, $SiO_2-Al_2O_3$).[23] Carbonylation rates are strictly proportional to the number of H^+ within 8-MR structures in FER and MOR, which varied with Na^+ content and sample provenance and was measured by deconvolution of OH infrared bands and by titration of 12-MR H^+ with large molecules (n-hexane, pyridine, 2,6-lutidine).[23] Carbonylation rates were independent of the number of protons within 10-MR or 12-MR structures, in spite of acid strengths (ΔE_{DP}) that do not depend on location.[11]

Thus, the preferential stabilization of carbonylation transition states within 8-MR voids cannot reflect the electrostatic component of ion-pair energies. Theoretical estimates of barriers for CO addition to bound CH_3 are similar at all four Al T-site locations within MOR when the methods used account for electrostatic, but not attractive dispersion forces; yet, values are ~30 kJ/mol lower within 8-MR voids using ab initio[24] or density functional theory (DFT)-based methods[25] that account for dispersion. More effective van der Waals interactions within smaller voids decrease the enthalpies of transition states, as long as they fit, relative to larger voids. Although tighter confinement causes entropy losses, activation free energies are smaller and turnover rates larger within 8-MR voids at the low temperatures of DME carbonylation catalysis.

Entropic Benefits of Partial Confinement in Catalysis at High Temperatures

Monomolecular alkane cracking and dehydrogenation prevail at high temperatures (>623 K) and low pressures of alkene products.[26] They involve cations with $(C-C-H)^+$ or

$(C-H-H)^+$ character that mediate kinetically-relevant C−C or C−H bond scissions (Scheme 1) and form via proton transfer to physisorbed alkanes present at low intrazeolite concentrations ($C_{A(z)}$) during catalysis.[14] Turnover rates (per H^+) are given by

$$r = k_{int}\, C_{A(z)} = k_{int}\, K_{ads} P_A = k_{meas}\, P_A \quad (2)$$

where K_{ads} is the alkane adsorption equilibrium constant and k_{int} is the rate constant for C−C or C−H scission steps (Scheme 1). Measured rate constants (k_{meas}) reflect free energy differences between transition states stabilized within voids and gaseous alkanes:

$$k_{meas} = (k_B T/h) \exp\left(-(\Delta G^\circ_{\ddagger} - \Delta G^\circ_{A(g)} - \Delta G^\circ_{H^+Z^-})/RT \right) \quad (3)$$

Measured activation energies (E_{meas}) depend on intrinsic activation barriers (E_{int}) and adsorption enthalpies (ΔH_{ads}):

$$E_{meas} = E_{int} + \Delta H_{ads} = \Delta H^\circ_{\ddagger} - \Delta H^\circ_{H^+Z^-} - \Delta H^\circ_{A(g)} \quad (4)$$

and reflect enthalpy differences between transition states and gaseous alkanes. Analogous relations hold for activation entropies (ΔS_{meas}) derived from pre-exponential factors:

$$\Delta S_{meas} = \Delta S_{int} + \Delta S_{ads} = \Delta S^\circ_{\ddagger} - \Delta S^\circ_{H^+Z^-} - \Delta S^\circ_{A(g)} \quad (5)$$

Monomolecular cracking and dehydrogenation rate constants were larger (by factors of 3−17; 748 K) on 8-MR than 12-MR protons in MOR for propane, *n*-butane, and isobutane reactants,[14,15] as also found for DME carbonylation.[23] These alkanes (~0.65−0.83 nm in length), however, cannot be fully contained within shallow 8-MR pockets (~0.37 nm deep); indeed, 8-MR H^+ sites preferentially cleave the terminal C−C bonds in *n*-butane.[14] Activation energies (E_{meas}) were larger, and activation entropies (ΔS_{meas}) were less negative for propane cracking in 8-MR than 12-MR locations (Table 1). Partial containment precludes effective van der Waals contacts between pore walls and organic cations at the transition state, causing them to retain larger amounts of gaseous reactant entropy at the expense of enthalpic stability. Turnover rates are higher when cations are partially confined because entropy becomes a dominant term in activation free energies at the high temperatures of alkane activation.

SCHEME 1. Monomolecular Alkane Activation on Brønsted Acid Sites[a]

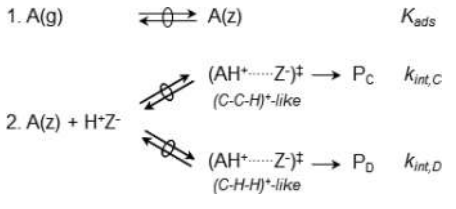

[a](1) Gaseous alkanes (A(g)) and those adsorbed (A(z)) onto acid sites within zeolite voids (H^+Z^-) are quasi-equilibrated. (2) Kinetically-relevant cracking or dehydrogenation via carbonium-ion-like transition states to form products (P_C, P_D) depicted using transition state theory formalism.

Partial Confinement Effects on Alkane Cracking and Dehydrogenation Selectivities

As the fraction of sites in 8-MR MOR pockets increased, cracking-to-dehydrogenation ratios *decreased* for propane and *n*-butane but *increased* for isobutane (Figure 1), despite analogous elementary steps for all reactants. For a given alkane, cracking-to-dehydrogenation ratios solely reflect differences in stability between the two transition states:

$$k_{meas,C}/k_{meas,D} = \exp\left(-(\Delta G^\circ_{\ddagger,C} - \Delta G^\circ_{\ddagger,D})/RT \right) \quad (6)$$

Thus, partial confinement preferentially stabilizes transition states for *n*-alkane dehydrogenation (relative to *n*-alkane cracking) and isobutane cracking (relative to isobutane dehydrogenation). The location of protons within different voids of the same zeolite structure influences turnover rates for monomolecular reactions of a given alkane (Table 1), but to different extents as these ratios show (Figure 1).

Kinetic preferences between cracking and dehydrogenation in 8-MR MOR pockets depend on alkane structure and enable changes in reaction selectivity, but on a phenomenological basis that prevents predictions for other alkanes or void structures. Why do transition states so similar in structure sense confinement so differently and why does this sensitivity depend so strongly on whether alkanes are linear or branched? While rate constant ratios depend only on free

TABLE 1. Measured Rate Constants, Activation Energies, Entropies, and Free Energies (748 K) for Monomolecular Propane Cracking on 8-MR and 12-MR H^+ Sites of MOR Zeolites[14]

location	k_{meas} ($/10^{-3}$) (mol (mol(H^+)·s·bar)$^{-1}$)	E_{meas} (kJ mol^{-1})	ΔS_{meas} (J mol^{-1} K^{-1})	ΔG_{meas} (kJ mol^{-1})
8-MR	2.0 ± 0.5	164 ± 5	−91 ± 9	227 ± 2
12-MR	0.7 ± 0.4	151 ± 5	−117 ± 14	234 ± 3

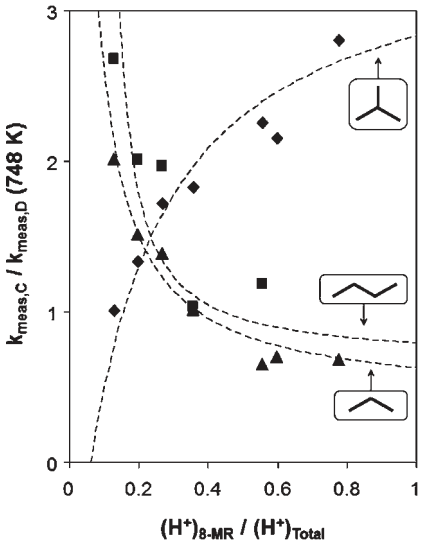

FIGURE 1. Monomolecular cracking-to-dehydrogenation rate constant ratios (748 K) for propane (▲), *n*-butane (■), and isobutane (◆) versus 8-MR H^+ fraction in MOR. Dashed curves represent ratios expected from 8-MR and 12-MR rate constants reported elsewhere.[14,15]

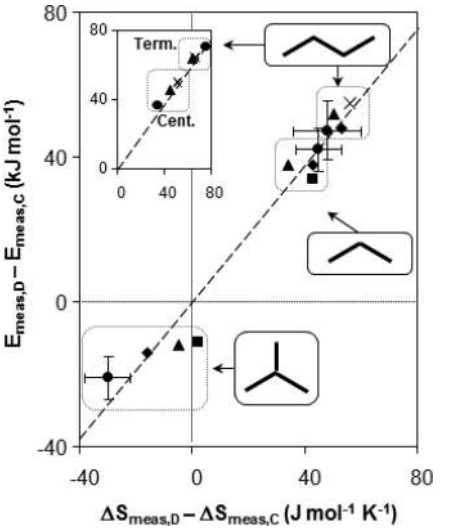

FIGURE 2. Differences in measured activation energies (E_{meas}) and entropies (ΔS_{meas}) between monomolecular alkane (propane, *n*-butane, isobutane) dehydrogenation and cracking on MOR (◆), MFI (●), FER (▲), USY (■), and chemically dealuminated-USY (x). Error bars shown for MFI are representative of errors for all samples. Dashed line represents least-squares regression. Inset: *n*-butane cracking at terminal and central C–C bonds.

energy differences between the two transition states involved (eq 6), each contain enthalpy and entropy terms that can be obtained independently from temperature effects on cracking and dehydrogenation rates. The catalytic consequences of enthalpy–entropy trade-offs imposed by confinement differ for two transition states accessible to each reactant because of how late they occur along their reaction coordinates, a property that is reflected in their respective activation barriers, as we discuss next.

Relations Between Ion-Pair Enthalpy and Entropy

Figure 2 shows differences in activation *energy* between dehydrogenation and cracking versus activation *entropy* differences for each alkane (propane, *n*-butane, isobutane) on each zeolite (FER, MFI, MOR, USY, CD-USY (chemically dealuminated-USY using $(NH_4)_2SiF_6$)). For a given alkane and zeolite, E_{meas} (or ΔS_{meas}) values for dehydrogenation and cracking differ only because their transition states differ in enthalpy (or entropy):

$$E_{meas,D} - E_{meas,C} = \Delta H^{\circ}_{\ddagger,D} - \Delta H^{\circ}_{\ddagger,C} \qquad (7)$$

Barriers were *larger* for dehydrogenation than for cracking for propane and *n*-butane, but *smaller* for isobutane (Figure 2). Thus, *n*-alkane dehydrogenation ion-pairs are higher in enthalpy than for cracking, but the opposite applies to isobutane. *n*-Alkane dehydrogenation and isobutane cracking also gave less negative ΔS_{meas} values than their respective counterparts (Figure 2), in turn, indicating that higher enthalpy ion-pairs also have larger entropies.

These data and their implications for ion-pair enthalpy–entropy trade-offs are consistent with charge transfer reaction coordinates based on reactant and product potentials (Scheme 2).[27,28] In this approach, paths from one reactant to several products differ only because of product energies. Transition states for the higher barrier path occur later along reaction coordinates and more closely resemble products. For monomolecular alkane activation, products contain one more molecule than reactants, and later transition states become looser and higher in entropy. As a result, ion-pairs that are higher in enthalpy are also higher in entropy.

For each alkane, rates of the higher barrier reaction selectively increased when transition states were partially confined within 8-MR MOR pockets (Figure 1), despite their weaker enthalpic stabilization compared with full confinement within 12-MR channels. The different kinetic preferences of cracking and dehydrogenation predominantly reflect entropic effects of partial confinement, which become more consequential for stability with increasing temperature and for looser transition states. Enthalpy and entropy differences between cracking and dehydrogenation transition states reflect differences in structure between $(C–C–H)^+$ and $(C–H–H)^+$ cations formed as C–C and C–H

SCHEME 2. Energy Diagrams for Two Reactions of One Alkane, Adapted from Charge Transfer Reaction Coordinates[a]

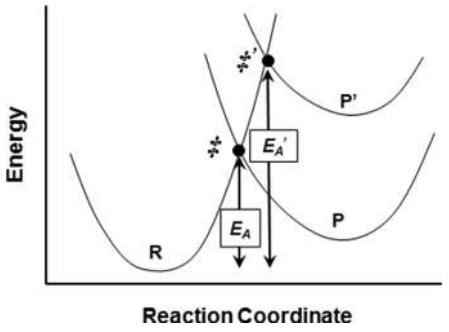

[a]Transition states (‡, ‡′) determined from intersections between reactant (R) and product (P, P′) potentials. Arrows denote activation barriers (E_A, E_A').

SCHEME 3. Thermochemical Cycles of Measured Activation Energies and Entropies for Monomolecular Alkane Reactions at Zeolitic Acid Sites[a]

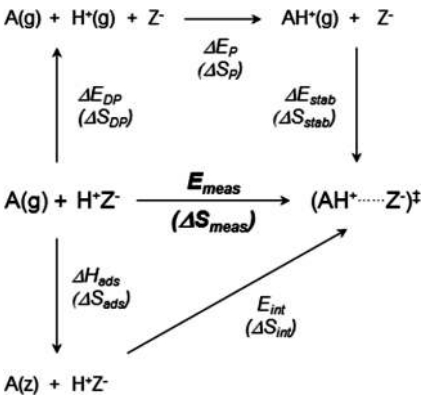

[a]Measured activation energies (E_{meas}) and entropies (ΔS_{meas}) depend on quasi-equilibrated alkane adsorption (ΔH_{ads}, ΔS_{ads}) at zeolitic acid sites (H^+Z^-) and kinetically-relevant protonation (E_{int}, ΔS_{int}) steps. They reflect contributions from deprotonation (ΔE_{DP}, ΔS_{DP}), gas-phase alkane protonation (ΔE_P, ΔS_P), and stabilization of gaseous cations within zeolite voids (ΔE_{stab}, ΔS_{stab}).

bonds acquire positive charge. These differences are intrinsic to reactant molecules and independent of zeolite structure (Figure 2). We examine next how reactant and catalyst properties influence the entropy and enthalpy terms in activation free energies for Brønsted acid catalysis using thermochemical cycles that dissect free energies into their fundamental components.

Born–Haber Thermochemical Cycles for Monomolecular Alkane Reactions

Scheme 3 depicts a thermochemical cycle that describes energies and entropies of ion-pairs formed from gaseous alkanes (E_{meas}, ΔS_{meas}) via adsorption (ΔH_{ads}, ΔS_{ads}) and subsequent proton transfer (E_{int}, ΔS_{int}). It includes a hypothetical path to these transition states involving deprotonation

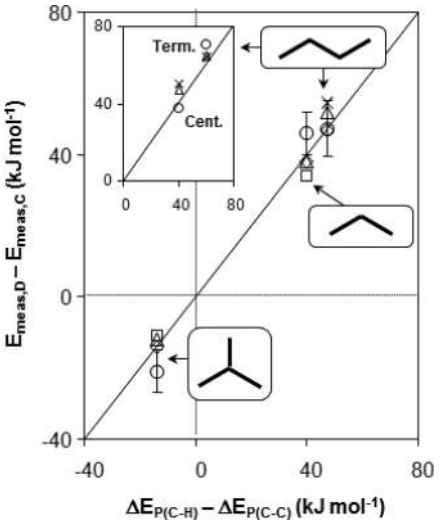

FIGURE 3. Difference between measured activation energies (E_{meas}) for monomolecular alkane dehydrogenation and cracking on MOR (◇), MFI (○), FER (△), USY (□) and chemically dealuminated-USY (x) versus the difference between bond-averaged gas-phase C–H and C–C proton affinities (ΔE_P) of propane, *n*-butane, and isobutane. Error bars shown for MFI are representative of errors for all samples. Equation 11 plotted as solid line. Inset: *n*-butane cracking at terminal and central C–C bonds.

of the acid, protonation of C–C or C–H bonds in gaseous alkanes, and electrostatic and van der Waals stabilization of the gaseous cations within zeolite voids. Measured activation energies and entropies are given by

$$E_{meas} = \Delta E_{DP} + \Delta E_P + \Delta E_{stab} \quad (8)$$

$$\Delta S_{meas} = \Delta S_{DP} + \Delta S_P + \Delta S_{stab} \quad (9)$$

Here, ΔE_{DP} is the deprotonation energy, ΔE_P is the gas-phase affinity of alkane C–C or C–H bonds for protonation, and ΔE_{stab} is the stabilization energy; the analogous ΔS terms in eq 9 describe measured activation entropies.

Acid site deprotonation reflects only catalyst properties and requires that Z–H bonds cleave heterolytically and H^+ and Z^- fragments separate to noninteracting distances; ΔE_{DP}[10–12] and ΔS_{DP} values are independent of active site location. Gas-phase protonation of alkane C–C or C–H bonds forms carbonium-ion-like complexes, with ΔE_P and ΔS_P values that depend on proton location within the cation but not on any catalyst properties. The confinement of gaseous cations or reactants within voids depends on both catalyst and reactant properties. Cations are stabilized (ΔE_{stab}, ΔS_{stab}) via electrostatic interactions with the anionic framework and, to a lesser extent, via van der Waals forces, while neutral alkanes are predominantly stabilized by the latter (ΔH_{ads}, ΔS_{ads}).[17–19]

Gas-Phase Alkane Proton Affinities Determine Monomolecular Activation Barriers

Differences in cracking and dehydrogenation barriers (eq 8) are given by

$$E_{meas,D} - E_{meas,C} = (\Delta E_{DP,D} + \Delta E_{P,D} + \Delta E_{stab,D}) - (\Delta E_{DP,C} + \Delta E_{P,C} + \Delta E_{stab,C}) \quad (10)$$

ΔE_{DP} terms rigorously cancel when both reactions occur on the same acid. Confinement stabilizes gaseous analogues of both transition states to similar extents (ΔE_{stab}), because of their similar charge (+0.8−0.9e) and its distribution,[5−7,29] which define electrostatic effects, and their similar size, which determines van der Waals contacts. Thus, cracking and dehydrogenation barriers for a given alkane and zeolite differ predominantly because C−C and C−H bond proton affinities are different:

$$E_{meas,D} - E_{meas,C} = \Delta E_{P,D} - \Delta E_{P,C} \quad (11)$$

The carbonium-ions formed upon protonation of gaseous alkanes decompose without detectable barriers to form complexes containing a neutral fragment (smaller alkane or H_2) and a carbenium ion interacting via van der Waals forces with each other,[30−33] similar to the late transition state structures identified by theory.[29,34−36]

Indeed, differences between cracking and dehydrogenation barriers for each alkane agree with proton affinity differences between their respective C−C and C−H bonds (Figure 3), properly weighted by the number of each bond (details in the Supporting Information).[15] Activation energies were higher for terminal than central C−C cleavage in *n*-butane (Figure 3 inset), consistent with the higher energy $(C-C-H)^+$ cations formed at terminal locations (by 20−25 kJ/mol) as determined by ab initio methods.[32,37] Activation entropies are also higher for terminal than central cracking (Figure 2 inset), consistent with the higher enthalpy ion-pairs for terminal scission being later and looser (Scheme 2). Next, we examine how the structures of alkanes influence the entropies of their cracking transition states and cause differences between terminal and central bonds of *n*-butane and among C_3−C_6 *n*-alkanes.

Effects of *n*-Alkane Size on Monomolecular Cracking Turnover Rates

Measured rate constants (773 K) for monomolecular cracking of C_3−C_6 *n*-alkanes on H-MFI increase markedly (>100-fold) with chain size; these rate constants reflect the cracking of all

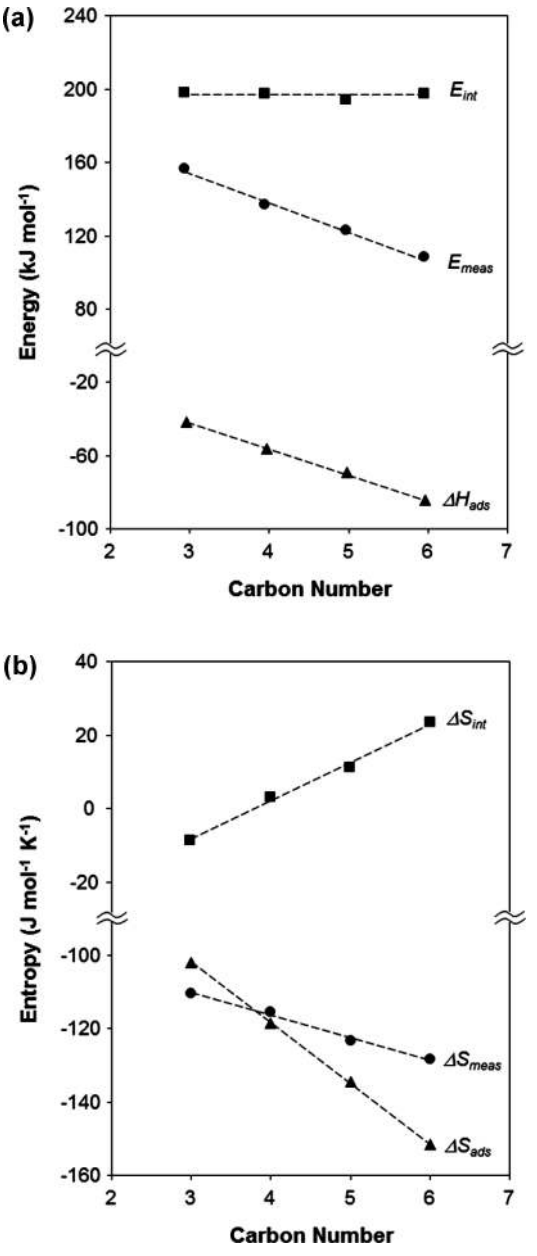

FIGURE 4. (a) Energy and (b) entropy terms in adsorption constants[18,19] (▲), and measured[38] (●) and intrinsic (■) rate constants for monomolecular cracking of *n*-alkanes on MFI.

C−C bonds in the reactant and thus their reactivity-average.[38] *n*-Alkane adsorption constants (K_{ads}) at reaction temperatures can be estimated from adsorption enthalpies and entropies, which depend weakly on temperature:[39−41]

$$K_{ads} = \exp(-(\Delta H_{ads} - T\Delta S_{ads})/RT) \quad (12)$$

Adsorption constants (773 K),[39] from eq 12 and values of ΔH_{ads} and ΔS_{ads} (measured at 353 K),[18,19] vary less than 2-fold among C_3−C_6 *n*-alkanes. Ab initio statistical thermodynamics methods (<5-fold)[40] and

configurational-bias Monte Carlo simulations (<2-fold)[42,43] give a similar range of values.

Intrinsic rate constants (773 K), determined from these adsorption constants and eq 2 and corrected for the number of C−C bonds, increased monotonically with alkane size and were ~50 times larger for *n*-hexane than for propane.[39] Intrinsic activation barriers, which reflect energy differences between transition states and physisorbed alkanes, depend on energies for the corresponding hypothetical steps in Scheme 3:

$$E_{int} = \Delta E_{DP} + \Delta E_P + \Delta E_{stab} - \Delta H_{ads} \quad (13)$$

Dispersive interactions stabilize reactants and transition states, which differ only in the presence of a single proton, to similar extents. They account for the effects of alkane size on ΔH_{ads} and E_{meas} (via ΔE_{stab}); both terms decrease in parallel for C_3-C_6 *n*-alkanes in H-MFI (12−16 kJ/mol per CH_2 group; Figure 4a). Alkane size does not affect ΔE_{DP}; moreover, its influence on ΔE_P, for which there are small differences with C−C bond position,[37] is attenuated because E_{meas} values reflect reactivity-averaged C−C scission events. Differences in *n*-alkane (or channel) size predominantly influence the number (or strength) of van der Waals contacts with pore walls, but in a commensurate manner for both reactants and transition states; thus, intrinsic barriers are similar for C_3-C_6 *n*-alkanes (194−198 kJ/mol; Figure 4a) on H-MFI[38] and insensitive to zeolite structure for C_3H_8 cracking.[14,44]

The higher intrinsic rate constants for larger *n*-alkanes reflect higher transition state entropies relative to alkanes physisorbed on acid sites (ΔS_{int}; Figure 4b).[39,40] This increase reflects ΔS_{ads} and ΔS_{meas} terms that, in contrast with ΔH_{ads} and E_{meas} (Figure 4a), decrease to different extents with increasing alkane size (~17 and ~6 J/mol·K per CH_2 group in H-MFI, respectively; Figure 4b). Intrinsic activation entropies can be described using the hypothetical steps in Scheme 3:

$$\Delta S_{int} = \Delta S_{DP} + \Delta S_P + \Delta S_{stab} - \Delta S_{ads} \quad (14)$$

Confinement causes entropy losses because attractive van der Waals interactions restrict mobility. We *surmise* that dispersive interactions similarly influence entropies of *n*-alkanes (ΔS_{ads}) and their transition states (ΔS_{stab}), in view of their similar size, using arguments similar to those that account for the similar van der Waals contributions to their enthalpies. Confinement *may* cause entropy differences between charged transition states and neutral reactants *if* electrostatic interactions with the anionic framework change the amount or distribution of charge in the cation. Such perturbations seem inconsistent with nearly full proton transfer (+0.8−0.9e) and with the local nature of this charge in both transition state[5−7,29,30] and gaseous[30−33] complexes; in turn, these entropy changes (contained within ΔS_{stab}) are small and insensitive to *n*-alkane size. Chain length must therefore cause differences in the entropy gained upon protonation of C−C bonds in gaseous alkanes (ΔS_P), even in the absence of concomitant effects on protonation enthalpies (ΔE_P).[37] These entropy gains reflect the emergence of frustrated rotational and translational modes accessible at late transition states, but not in intact neutral alkanes.

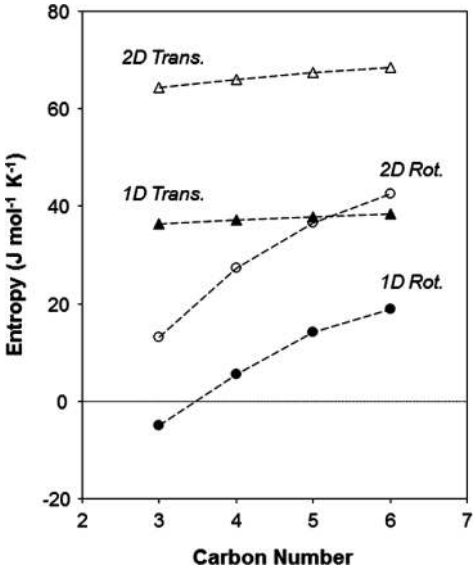

FIGURE 5. Entropy differences between transition states and physisorbed reactants in *n*-alkane cracking caused by gaining 1D (●) and 2D (○) rotation and 1D (▲) and 2D (△) translation; estimated using statistical mechanics for scission of individual C−C bonds and weighted for the number of such bonds in each *n*-alkane.

Entropic Consequences of Chain Size in Monomolecular Alkane Cracking

Ab initio treatments indicate that low-frequency vibrations in alkanes physisorbed at intrazeolitic protons represent frustrated translations and rotations relative to the confining walls.[40,41] The entropies of these modes were estimated by statistical mechanics formalisms that treat alkane translation on a plane perpendicular to the O−H bond axis (2D free translation) and rotation about their center axis (1D free rotation); rotation can also occur about an axis perpendicular to the zeolite surface (2D free rotation) when void spaces permit.[40,41] Late cracking transition states resemble van der

Waals complexes formed by charge separation and C–C bond lengthening.[5,29,34] Distortion of internal bond lengths and angles in these complexes represent hindered rotations and rocking vibrations of two fragments stabilized weakly by dispersion forces; these motions are essentially barrierless compared to the much larger reaction barriers that predominantly reflect the energies required for charge separation.[6,7,29,45–50] We expect the statistical thermodynamic treatments used for confined alkanes[40,41] would also accurately estimate entropies for late transition states, in which the two products are nearly formed.

Entropy gains along the path from *n*-alkanes to two molecules were calculated for each C–C bond cleavage event, separately for one and two degrees of free translational and rotational freedom (details in the Supporting Information); bond-averaged values are shown in Figure 5 as a function of chain size. The formation of two molecules causes large translational entropy gains (~37 (1D), ~66 (2D) J/mol·K) that are, however, affected only *weakly* by alkane size (4 J/mol·K per CH_2 group (2D)). In sharp contrast, rotational entropy gains depend *strongly* on chain size (~22 (1D), ~30 (2D) J/mol·K per CH_2 group). Entropy gains from 1D free rotation (Figure 5) are similar to ΔS_{int} values for each *n*-alkane (Figure 4b); they are also higher for terminal than central C–C cleavage in *n*-butane (by 8 J/mol·K), consistent with the higher activation entropies measured for terminal cracking (Figure 2 inset). The quantitative agreement between these data suggest that *if* fragments at late transition states rotate freely relative to one another, other translational and rotational modes do not significantly contribute to ΔS_{int} values. Irrespective of the detailed modes and their specific barriers at transition states, however, new rotational modes appear to cause the increases in ΔS_{int} and k_{int} values with *n*-alkane size. These effects resemble those for protonation[51] and radical dissociation[52] of gaseous hydrocarbons, which disrupt internal symmetry and create new rotations that cause entropy gains.

Thermochemical relations provide predictive insights into chemical reactivity and selectivity by rigorously connecting thermodynamic properties of transition states to those of reactants and catalysts. As *n*-alkanes become larger in size, reactant rotational entropies and cracking turnover rates increase concomitantly. Proton affinity differences between alkane C–C and C–H bonds vary with reactant size and structure, leading to commensurate enthalpy differences between monomolecular cracking and dehydrogenation transition states. The selectivity toward breaking these bonds, in turn, depends on local void structure; higher energy ion-pairs, which are also later and looser, are preferentially stabilized within voids that confine them partially. Tighter confinement results in larger enthalpy gains, at the expense of entropy, and benefits DME carbonylation transition states at low temperatures (400–500 K); however, looser confinement and larger entropies, at the expense of enthalpy, benefit late monomolecular alkane transition states at high temperatures (700–800 K). In contrast to monomolecular routes, bimolecular alkene reactions (alkylation, hydrogenation, oligomerization) require that two reactants *lose* entropy to form loosely bound ion-pairs at *early* transition states, yet the entropic gains associated with partial ion-pair confinement are similarly consequential for turnover rates of these reactions at high temperatures.[53,54]

Outlook

These ubiquitous principles for catalysis within confined spaces generate research inquiries accessible to theory and experiment. Opportunities emerge for designing catalytic materials with active sites located within voids that provide the "right fit" for a given chemical transformation. Active site distributions can be modified by postsynthetic treatments, but how do we synthesize materials with sites already in desired locations? Recent studies of FER zeolites have demonstrated precise control of Al siting at specific framework locations using structure-directors that template different voids during synthesis.[55,56] These findings offer promise for the development of related strategies to control heteroatom siting in other microporous frameworks.

Identifying proton locations within different voids of a given structure, even before and after catalytic reactions, remains a state-of-the-art process. Proton locations can be determined accurately when OH groups differ in infrared vibrational frequencies, in their ability to interact with titrants of different size, and in their preference for exchange with other cations.[23] These methods provide unclear inferences for structures with many different Al T-sites within voids that differ only slightly in size, such as MFI. Nuclear magnetic resonance spectroscopic methods can resolve Al atoms with different isotropic chemical shifts in MFI, but the specific assignment to unique T-site locations remains uncertain.[57] Methods to characterize Al or OH location with increasing accuracy will require synergistic approaches using experiment and theory, in which theoretical methods treat spectral features more definitively and help guide experimental design.

Theoretical chemistry can probe how and why voids solvate intermediates and transition states. Attractive dispersion forces largely account for catalytic enhancements caused by confinement and for reactivity differences among zeolites with diverse void structures but acid sites of similar strength. Thus, ab initio[24,40,41] and DFT-based methods that account for dispersion[50] are essential to describe reaction coordinate and *potential energy* surfaces within confined spaces. These reaction coordinates exist, however, within *free energy* surfaces; therefore, entropies of confined species need also be determined accurately to predict reactivity. Classical mechanics seem unable to accurately describe low-frequency vibrations, such as hindered rotations,[46,47] which are essential to describe entropy differences between intact molecules and ion-pairs at transition states. Treatment of low-frequency vibrations instead as free rotational and translational modes using statistical thermodynamics formalisms has estimated entropies of physisorbed alkanes that resemble experimentally determined values.[40,41,58]

The choice and design of microporous voids for specific catalytic targets typically relies on criteria based on size exclusion, despite the strong consequences of confinement for transition state stability. This reflects our emerging knowledge about the specific catalyst and reactant properties that influence turnover rates and selectivities. These insights become increasingly important as we expand the ranges of materials used and of the reactions they catalyze. Predictive guidance based on rigorous mechanistic interpretation can replace phenomenological considerations of void geometry and topology and enable the design of inorganic structures that mimic biological catalysts in their ability to confine specific transition states and selectively catalyze the chemical reactions that they mediate.

Summary

Turnover rates and selectivities in zeolite acid catalysis depend predominantly on enthalpic and entropic stabilities of ion-pair transition states at low and high temperatures, respectively. The catalytic consequences of reactant and void structure are identified using thermochemical cycles that dissect activation energies and entropies into terms that depend differently on reactant and catalyst identity. These findings provide insight into the high specificity of both DME carbonylation (400−500 K) and monomolecular alkane activation (700−800 K) turnovers for 8-MR MOR pockets, the higher selectivities to *n*-alkane dehydrogenation but isoalkane cracking in such locations, and the marked increase in cracking turnover rates with *n*-alkane size.

Supporting Information. Estimation of alkane gas-phase proton affinities and entropies of hydrocarbons adsorbed within zeolite voids. This material is available free of charge via the Internet at http://pubs.acs.org.

BIOGRAPHICAL INFORMATION

Rajamani Gounder received his B.S. in Chemical Engineering from the University of Wisconsin in 2006, where he performed undergraduate research under Professor James A. Dumesic. His research and teaching at Berkeley have been recognized with the Heinz Heinemann Award for Graduate Research in Catalysis (2010) and the Dow Excellence in Teaching Award (2010). Upon completion of his doctoral dissertation at Berkeley, he will conduct postdoctoral research with Professor Mark E. Davis at the California Institute of Technology.

Enrique Iglesia is the Theodore Vermeulen Chair in Chemical Engineering at the University of California, Berkeley and a Faculty Senior Scientist at the E. O. Lawrence Berkeley National Laboratory. He received his Ph.D. in Chemical Engineering in 1982 from Stanford University. In 1993, he joined the Berkeley faculty after 11 years at Exxon Research and Engineering. He is the Director of the Berkeley Catalysis Center, the President of the North American Catalysis Society, and the former Editor-in-Chief of *Journal of Catalysis* (1997−2010). His research interests include the synthesis and structural and mechanistic characterization of inorganic solids useful as catalysts for chemical reactions important in energy conversion, petrochemical synthesis, and environmental control.

Financial support from the Chevron Energy Technology Company is acknowledged.

FOOTNOTES

*To whom correspondence should be addressed. E-mail: iglesia@berkeley.edu.

REFERENCES

1 Degnan, T. F. The implications of the fundamentals of shape selectivity for the development of catalysts for the petroleum and petrochemical industries. *J. Catal.* **2003**, *216*, 32–46.
2 Venuto, P. B. Organic catalysis over zeolites: A perspective on reaction paths within micropores. *Microporous Mater.* **1994**, *2*, 297–411.
3 Corma, A. Inorganic solid acids and their use in acid-catalyzed hydrocarbon reactions. *Chem. Rev.* **1995**, *95*, 559–614.
4 Kazansky, V. B. The nature of adsorbed carbenium ions as active intermediates in catalysis by solid acids. *Acc. Chem. Res.* **1991**, *24*, 379–383.
5 van Santen, R. A.; Kramer, G. J. Reactivity theory of zeolitic Brønsted acidic sites. *Chem. Rev.* **1995**, *95*, 637–660.
6 Rigby, A. M.; Kramer, G. J.; van Santen, R. A. Mechanisms of hydrocarbon conversion in zeolites: A quantum mechanical study. *J. Catal.* **1997**, *170*, 1–10.
7 Frash, M. V.; van Santen, R. A. Quantum-chemical modeling of the hydrocarbon transformations in acid zeolite catalysts. *Top. Catal.* **1999**, *9*, 191–205.
8 Koppel, I. A.; Burk, P.; Koppel, I.; Leito, I.; Sonoda, T.; Mishima, M. Gas-phase acidities of some neutral Brønsted superacids: A DFT and ab initio study. *J. Am. Chem. Soc.* **2000**, *122*, 5114–5124.
9 Macht, J.; Carr, R. T.; Iglesia, E. Functional assessment of the strength of solid acid catalysts. *J. Catal.* **2009**, *264*, 54–66.
10 Eichler, U.; Brändle, M.; Sauer, J. Predicting absolute and site specific acidities for zeolite catalysts by a combined quantum mechanics interatomic potential function approach. *J. Phys. Chem. B* **1997**, *101*, 10035–10050.
11 Brändle, M.; Sauer, J. Acidity differences between inorganic solids induced by their framework structure. A combined quantum mechanics molecular mechanics ab initio study on zeolites. *J. Am. Chem. Soc.* **1998**, *120*, 1556–1570.

12 Sauer, J.; Sierka, M. Combining quantum mechanics and interatomic potential functions in ab initio studies of extended systems. *J. Comput. Chem.* **2000**, *21*, 1470–1493.

13 Bhan, A.; Iglesia, E. A link between reactivity and local structure in acid catalysis on zeolites. *Acc. Chem. Res.* **2008**, *41*, 559–567.

14 Gounder, R.; Iglesia, E. Catalytic consequences of spatial constraints and acid site location for monomolecular alkane activation on zeolites. *J. Am. Chem. Soc.* **2009**, *131*, 1958–1971.

15 Gounder, R.; Iglesia, E. Effects of partial confinement on the specificity of monomolecular alkane reactions for acid sites in side pockets of mordenite. *Angew. Chem., Int. Ed.* **2010**, *49*, 808–811.

16 Carr, R. T.; Neurock, M.; Iglesia, E. Catalytic consequences of acid strength in the conversion of methanol to dimethyl ether. *J. Catal.* **2011**, *278*, 78–93.

17 Eder, F.; Lercher, J. A. On the role of the pore size and tortuosity for sorption of alkanes in molecular sieves. *J. Phys. Chem. B* **1997**, *101*, 1273–1278.

18 Eder, F.; Lercher, J. A. Alkane sorption in molecular sieves: The contribution of ordering, intermolecular interactions, and sorption on Brønsted acid sites. *Zeolites* **1997**, *18*, 75–81.

19 Eder, F.; Stockenhuber, M.; Lercher, J. A. Brønsted acid site and pore controlled siting of alkane sorption in acidic molecular sieves. *J. Phys. Chem. B* **1997**, *101*, 5414–5419.

20 Savitz, S.; Siperstein, F.; Gorte, R. J.; Myers, A. L. Calorimetric study of adsorption of alkanes in high-silica zeolites. *J. Phys. Chem. B* **1998**, *102*, 6865–6872.

21 Cheung, P.; Bhan, A.; Sunley, G. J.; Iglesia, E. Selective carbonylation of dimethyl ether to methyl acetate catalyzed by acidic zeolites. *Angew. Chem., Int. Ed.* **2006**, *45*, 1617–1620.

22 Cheung, P.; Bhan, A.; Sunley, G. J.; Law, D. J.; Iglesia, E. Site requirements and elementary steps in dimethyl ether carbonylation catalyzed by acidic zeolites. *J. Catal.* **2007**, *245*, 110–123.

23 Bhan, A.; Allian, A. D.; Sunley, G. J.; Law, D. J.; Iglesia, E. Specificity of sites within eight-membered ring zeolite channels for carbonylation of methyls to acetyls. *J. Am. Chem. Soc.* **2007**, *129*, 4919–4924.

24 Neurock, M. Engineering molecular transformations for sustainable energy conversion. *Ind. Eng. Chem. Res.* **2010**, *49*, 10183–10199.

25 Boronat, M.; Martinez, C.; Corma, A. Mechanistic differences between methanol and dimethyl ether carbonylation in side pockets and large channels of mordenite. *Phys. Chem. Chem. Phys.* **2011**, *13*, 2603–2612.

26 Haag, W. O.; Dessau, R. M. Duality of mechanism for acid-catalyzed paraffin cracking. *Proc. 8th Int. Congr. Catalysis. Berlin* **1984**, *2*, 305–316.

27 Marcus, R. A. Chemical and electrochemical electron-transfer theory. *Annu. Rev. Phys. Chem.* **1964**, *15*, 155–196.

28 Bell, R. P. *The proton in chemistry*; Chapman and Hall: London, 1973.

29 Zygmunt, S. A.; Curtiss, L. A.; Zapol, P.; Iton, L. E. Ab initio and density functional study of the activation barrier for ethane cracking in cluster models of zeolite H-ZSM-5. *J. Phys. Chem. B* **2000**, *104*, 1944–1949.

30 Collins, S. J.; O'Malley, P. J. Electronic structure studies of carbonium ions and their formation within acidic zeolites. *Top. Catal.* **1998**, *6*, 151–161.

31 Esteves, P. M.; Mota, C. J. A.; Ramírez-Solís, A.; Hernández-Lamoneda, R. Potential energy surface of the C_3H_9+ cations. Protonated propane. *J. Am. Chem. Soc.* **1998**, *120*, 3213–3219.

32 Esteves, P. M.; Alberto, G. G. P.; Ramírez-Solís, A.; Mota, C. J. A. The n-butonium cation (n-$C_4H_{11}+$): The potential energy surface of protonated n-butane. *J. Phys. Chem. A* **2000**, *104*, 6233–6240.

33 Mota, C. J. A.; Esteves, P. M.; Ramírez-Solís, A.; Hernández-Lamoneda, R. Protonated isobutane. A theoretical ab initio study of the isobutonium cations. *J. Am. Chem. Soc.* **1997**, *119*, 5193–5199.

34 Zheng, X. B.; Blowers, P. Reactivity of alkanes on zeolites: A computational study of propane conversion reactions. *J. Phys. Chem. A* **2005**, *109*, 10734–10741.

35 Zheng, X. B.; Blowers, P. Reactivity of isobutane on zeolites: A first principles study. *J. Phys. Chem. A* **2006**, *110*, 2455–2460.

36 Kazansky, V. B.; Frash, M. V.; van Santen, R. A. Quantum chemical study of the isobutane cracking on zeolites. *Appl. Catal., A* **1996**, *146*, 225–247.

37 Hunter, K. C.; East, A. L. L. Properties of C-C bonds in n-alkanes: Relevance to cracking mechanisms. *J. Phys. Chem. A* **2002**, *106*, 1346–1356.

38 Narbeshuber, T. F.; Vinek, H.; Lercher, J. A. Monomolecular conversion of light alkanes over H-ZSM-5. *J. Catal.* **1995**, *157*, 388–395.

39 Bhan, A.; Gounder, R.; Macht, J.; Iglesia, E. Entropy considerations in monomolecular cracking of alkanes on acidic zeolites. *J. Catal.* **2008**, *253*, 221–224.

40 De Moor, B. A.; Reyniers, M. F.; Gobin, O. C.; Lercher, J. A.; Marin, G. B. Adsorption of C_2-C_8 n-alkanes in zeolites. *J. Phys. Chem. C* **2011**, *115*, 1204–1219.

41 De Moor, B. A.; Reyniers, M. F.; Marin, G. B. Physisorption and chemisorption of alkanes and alkenes in H-FAU: A combined ab initio-statistical thermodynamics study. *Phys. Chem. Chem. Phys.* **2009**, *11*, 2939–2958.

42 Maesen, T. L. M.; Beerdsen, E.; Calero, S.; Dubbeldam, D.; Smit, B. Understanding cage effects in the n-alkane conversion on zeolites. *J. Catal.* **2006**, *237*, 278–290.

43 Swisher, J. A.; Hansen, N.; Maesen, T.; Keil, F. J.; Smit, B.; Bell, A. T. Theoretical simulation of n-alkane cracking on zeolites. *J. Phys. Chem. C* **2010**, *114*, 10229–10239.

44 Xu, B.; Sievers, C.; Hong, S. B.; Prins, R.; van Bokhoven, J. A. Catalytic activity of Brønsted acid sites in zeolites: Intrinsic activity, rate-limiting step, and influence of the local structure of the acid sites. *J. Catal.* **2006**, *244*, 163–168.

45 Janik, M. J.; Davis, R. J.; Neurock, M. A density functional theory study of the alkylation of isobutane with butene over phosphotungstic acid. *J. Catal.* **2006**, *244*, 65–77.

46 Bucko, T.; Benco, L.; Dubay, O.; Dellago, C.; Hafner, J. Mechanism of alkane dehydrogenation catalyzed by acidic zeolites: Ab initio transition path sampling. *J. Chem. Phys.* **2009**, *131*, 214508.

47 Bucko, T.; Hafner, J. Entropy effects in hydrocarbon conversion reactions: Free-energy integrations and transition-path sampling. *J. Phys.: Condens. Matter* **2010**, *22*, 384201.

48 Li, Q. B.; Hunter, K. C.; Seitz, C.; East, A. L. L. Geometry and torsional energies of a C-C-protonated n-alkane. *J. Chem. Phys.* **2003**, *119*, 7148–7155.

49 East, A. L. L.; Bucko, T.; Hafner, J. On the structure and dynamics of secondary n-alkyl cations. *J. Chem. Phys.* **2009**, *131*, 104314.

50 Mullen, G. M.; Janik, M. J. Density functional theory study of alkane-alkoxide hydride transfer in zeolites. *ACS Catal.* **2011**, *1*, 105–115.

51 East, A. L. L.; Smith, B. J.; Radom, L. Entropies and free energies of protonation and proton-transfer reactions. *J. Am. Chem. Soc.* **1997**, *119*, 9014–9020.

52 Benson, S. W. *Thermochemical kinetics*; John Wiley & Sons, Inc.: New York, 1976.

53 Gounder, R.; Iglesia, E. Catalytic hydrogenation of alkenes on acidic zeolites: Mechanistic connections to monomolecular alkane dehydrogenation reactions. *J. Catal.* **2011**, *277*, 36–45.

54 Gounder, R.; Iglesia, E. Catalytic alkylation routes via carbonium-ion-like transition states on acidic zeolites. *ChemCatChem* **2011**, *3*, 1134–1138.

55 Pinar, A. B.; Márquez-Álvarez, C.; Grande-Casas, M.; Pérez-Pariente, J. Template-controlled acidity and catalytic activity of ferrierite crystals. *J. Catal.* **2009**, *263*, 258–265.

56 Román-Leshkov, Y.; Moliner, M.; Davis, M. E. Impact of controlling the site distribution of Al atoms on catalytic properties in ferrierite-type zeolites. *J. Phys. Chem. C* **2011**, *115*, 1096–1102.

57 Sklenak, S.; Dedecek, J.; Li, C.; Wichterlová, B.; Gábová, V.; Sierka, M.; Sauer, J. Aluminium siting in the ZSM-5 framework by combination of high resolution Al-27 NMR and DFT/MM calculations. *Phys. Chem. Chem. Phys.* **2009**, *11*, 1237–1247.

58 De Moor, B. A.; Ghysels, A.; Reyniers, M. F.; Van Speybroeck, V.; Waroquier, M.; Marin, G. B. Normal mode analysis in zeolites: Toward an efficient calculation of adsorption entropies. *J. Chem. Theory Comput.* **2011**, *7*, 1090–1101.